Available online at www.sciencedirect.com
SCIENCE DIRECT
Journal of Power Sources 146 (2005) 418–422
JOURNAL OF POWER SOURCES
www.elsevier.com/locate/jpowsour

Low dimensional polymer electrolytes with enhanced Li^+ conductivities

Y. Zheng, J. Liu, Y.-P. Liao, G. Ungar, P.V. Wright *

Department of Engineering Materials, University of Sheffield, Mappin Street, Sheffield S1 3JD, UK

Available online 3 June 2005

Abstract

The structure of two amphiphilic low-dimensional copolymer electrolytes I of similar overall composition but prepared by different synthetic procedures is described. I are copolymers of poly [2,5,8,11,14-pentaoxapentadecamethylene(5-alkyloxy-1,3-phenylene)] (CmO5) and poly[2,-oxatrimethylene(5-alkyloxy-1,3-phenylene)] (CmO1) where the alkyl side chains having m carbons are mixed dodecyl/octadecyl (50/50). ^{1}H NMR shows that the copolymers have only 18 and 13% of CmO5 units in which $LiBF_4$ ions are separated by Li^+ encapsulation in tetraethoxy segments but molecular modelling suggests that in ionophobic CmO1 units the salt is mostly present as neutral aggregates *decoupled* from the polymer. Conductivities of microphase-separated mixtures with salt-bridge amphiphilic polyethers II and III of each system are similar. They have low temperature dependence over the range 20–110 °C at $\sim 10^{-3}$ S cm^{-1}. A conduction mechanism is proposed whereby Li^+ hopping takes place along rows of decoupled aggregates in an essentially *block* copolymer structure. Subambient measurements to −10 °C gave a conductivity of 4×10^{-5} S cm^{-1}.

Keywords: Copolymer characterisation; Decoupled salt aggregates; Molecular modelling; Conductivity

1. Introduction

Solvent-free polymer electrolytes are of considerable interest for lithium batteries in heavy-duty traction or aerospace applications where solvents present safety hazards [1] but ambient conductivities of conventional amorphous systems ($\sim 10^{-5}$ S cm^{-1}) [2] fall short of those realised in solvents or gels ($\sim 10^{-3}$ to 10^{-2} S cm^{-1}) [3]. Recent work [4–10] has shown that mixtures of lithium salts in self-organised lamellae of amphiphilic polymers having 5-alkoxy-3,4-phenylene units connected by oligoethoxy segments, I, with interphases of block copolymer II $-\{-[(CH_2)_4-O-]_{\sim 23}-(CH_2)_{12}-O-\}-$ give films having ambient conductivities $\sigma \sim 10^{-3}$ S cm^{-1} in impedance and extended dc polarisations between Li electrodes. The polymers I are abbreviated CmOn, where the number of side chain carbons $m = 12$, 16, and/or 18, and the number of skeletal oxygens $n = 1$–5.

In this paper we compare two synthetic procedures for I (methods X and Y) in which the halogens and hydroxyl functionalities of the base-catalysed 'Williamson' etherification are exchanged. The structures of the copolymers and the conductivities of microphase (deblended) mixtures I (X or Y):II:III:$LiBF_4$ where III is an ABA copolymer $C_{18}H_{37}-O-[-(CH_2)_4-O-]_{\sim 50}-C_{18}H_{37}$ ($M \cong 4000$) (Fig. 1) are also compared. Polymer III is a minor component (~8 wt.%) included so as to promote I/II interfacial stability [9,10]. The ionophobic terminal $-C_{18}H_{37}$ blocks should more readily manoeuvre alongside- and interact with the alkyl side chains at the lamellar surfaces of I than would the main-chain $-(CH_2)_{12}-$ blocks of II.

2. Experimental

2.1. General procedures

Dimethyl sulphoxide (DMSO) was dried and distilled before use. Other reagents were used without further purification. ^{1}H NMR was performed using a Bruker AC250 and GPC was carried out using a Hewlett-Packard 1090 liquid chromatograph. DSC was performed on Du Pont Instruments 910 and FT-IR Perkin-Elmer Spectrum 2000 scanning between 4000 and 400 cm^{-1}. Conductivity measurements were carried out using a Solartron 1287A

* Corresponding author.
E-mail address: p.v.wright@sheffield.ac.uk (P.V. Wright).

0378-7753/$ – see front matter © 2005 Elsevier B.V. All rights reserved.
doi:10.1016/j.jpowsour.2005.03.125

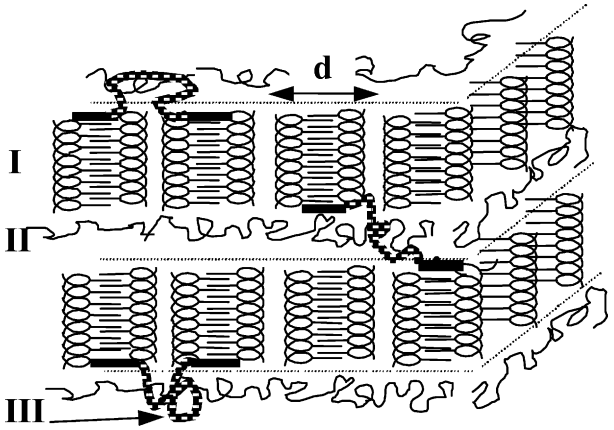

Fig. 1. Microphase structure of I:II:III:Li salt.

EI/1250 FRA (1 Hz–1 MHz, 100 mV amplitude) using indium-tin oxide (ITO) coated glass electrodes (resistance 40 Ω subtracted in Figs. 3 and 4) with a cellulose acetate or polyethylene spacer in an evacuated chamber. Molecular dynamics modelling was performed with Cerius^2 software with 'annealing cycles' between ambient and 600 K.

2.2. Synthesis of C12C18O5X(18%)

5-Dodecyloxy benzene-1,3-dimethanol (i), 5-octadecyloxy benzene-1,3-dimethanol (ia) and tetraethylene glycol dichloride were prepared as described previously [11]. C12C18O5X(18%), was prepared by heating 0.81 g (0.0025 mol) of i, 1.02 g (0.0025 mol) of ia and 1.16 g (0.005 mol) tetraethylene glycol dichloride, 2.24 g (0.04 mol) potassium hydroxide and 2.24 g potassium carbonate in 30 ml DMSO for 7 days at 90 °C under N_2. The polymer was precipitated in water, neutralized by addition of concentrated acetic acid and extracted into chloroform. After evaporation of chloroform, the residue was washed with hot water and finally with hot methanol. The product is pale brown. The FT-IR spectrum shows a medium ester C=O band at 1720 cm^{-1} GPC gave molar mass averages $<M_n>$ = 2614, $<M_w>$ = 52,541 and $<M_z>$ = 1,069,798. Melting point, 36 °C.

2.3. Method Y syntheses

1,3-Bis (bromomethyl)-5-dodecyl-oxybenzene (ii) and 1,3-bis (bromomethyl)-5-octadecyl-oxybenzene (iia) was prepared as described elsewhere [7].

C12C18O5Y(82%) was prepared by stirring ii (2 mmol), iia (2 mmol), tetraethyleneglycol (4 mmol), KOH (16 mmol) and DMSO (2.5 ml) at 60 °C under argon for 24 h and the temperature was raised to 80 °C for 4 days. The polymer was purified as above. Yield, 50% (1.4 g); (M_n = 9053, M_w = 28,906, M_z = 74,593). Melting point, 26 °C.

C12C18O5Y(6%) was prepared as above from ii (0.5 mmol), iia (0.5 mmol), i (0.3 mmol), ia (0.3 mmol), tetraethyleneglycol (0.4 mmol), KOH (4 mol), DMSO (2 ml). Yield, 46% (0.85 g); (M_n = 5145, M_w = 10,679, M_z = 19,243) Melting point, 33 °C.

C12C18O5Y(13%) 0.1 g of C12C18O5(82%), 0.45 g of C12C18O5(6%) and 0.1 g of iia were dissolved in chloroform and the solvent removed by evaporation. 0.024 g of KOH and 1 ml of DMSO were added and stirred at 85 °C under argon flow for 3 days during which the DMSO was progressively removed. The polymer was purified as above. Yield 0.5 g (91%); (M_n = 6460, M_w = 31,441, M_z = 285,654). Melting point, 35 °C.

Copolyether II $-\{-O-[-(CH_2)_4-O-]_{\sim 23}-(CH_2)_{12}-\}-$ ($<M_w> \cong 40$ k) and ABA block copolymer III $C_{18}H_{37}-O-[-(CH_2)_4-O-]_{\sim 50}-C_{18}H_{37}$ ($M \cong 3500$) were prepared as described previously [8].

In the four-component systems I:II:III:Li BF_4 (1:0.8:0.2:1.2) the molar ratio of salt refers to the repeat unit of I and the total mass of II plus III equalled the mass of I. The four-component blends were prepared from homogeneous dilute solutions of the mixtures in CH_2Cl_2/acetone by freeze-drying to fine powders. The solids were then fused under vacuum at 50 °C.

3. Results and discussion

3.1. Molecular structures of C12C18O5X(18%) and C12C18O5Y(13%)

^{1}H NMR data for the side chain and skeletal chain copolymers are given in Table 1. The total side chain signals correspond to 16 carbons consistent with 0.5/0.5 molar ratio mixture of $-(CH_2)_{12}-H$ and $-(CH_2)_{18}-H$ alkyls presumably arranged randomly along the chain. The multiple peaks at 3.65 ppm indicate the tetraethoxy content. Thus, in Scheme 1, p = 3/16 for C12C18O5X(18%) and p = 2/16 for C12C18O5Y(13%). The peaks at $\delta \sim 3.92$ correspond to the signals from the skeletal α-CH_2- (benzylic). In C12C18O5X(18%) they are present at only half of their

Table 1
^{1}H NMR data for C12C18O5 copolymers

	CH_3 alkyl	CH_2 alkyl	γ-CH_2 alkyl	β-CH_2 alkyl	CH_2 ethoxy	α-CH_2 alkyl	α-CH_2 benzyl	CH arom.
δ (ppm)	0.86	1.25	1.45	1.75	3.65	3.92	4.45	6.85–7.9
C12C18O5X(18%)	3, t	24, s	2, m	2, m	3, m	2, t	2, s	3 broad
C12C18O5Y(82%)	3, t	23, s	2, m	2, m	13, m	2, t	3.4, d	2.6, m
C12C18O5Y(6%)	3, t	23, s	2, m	2, m	1, m	2, t	3.5, d	3, m
C12C18O5Y(13%)	3, t	24, s	2, m	2, m	2, m	2, t	3.4, d	2.6, m

Numbers give the integrated proton signals for each chemical group. Letters refer to singlet (s), doublet (d), triplet (t) and multiple peaks (m).

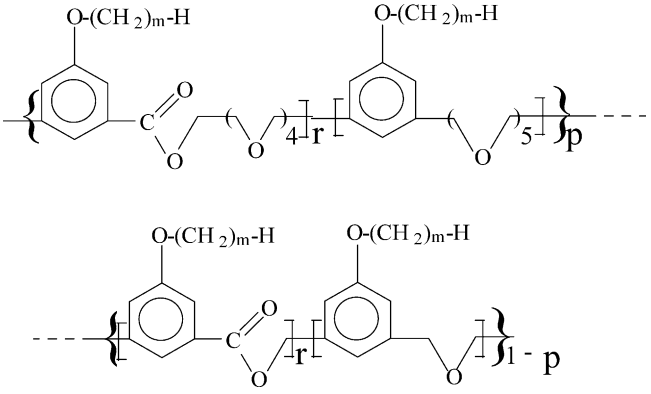

Scheme 1. Molecular structure of copolymers I.

expected intensity for a pure polyether. At the same time FT-IR suggests a strong ester C=O absorption at 1720 cm^{-1} and there are multiple ^1H NMR aromatic peaks between 6.9 and 7 ppm. These observations taken together suggest that C12C18O5X(18%) has a polyether–ester skeletal backbone with $r \sim 0.5$ in Scheme 1. For C12C18O5Y(13%) there are 3.4 skeletal α-CH_2− hydrogens and FT-IR of method Y products typically have negligible C=O bands suggesting that $r \sim 0.1$ or below.

3.2. Molecular dynamics modelling

Molecular dynamics models for complexes of the pure homopolymers C16O5:Li salt (1:1) and C16O1:$LiBF_4$ (2:1) are shown in Fig. 2(a) and (b). Experimental long spacings [9] from small-angle X-ray data (45 and 33 Å, respectively) are constraints to the models. It is apparent that in the C16O5 system ions are separated, the Li^+ being encapsulated within the tetraethoxy segments. In the C16O1 system, however, ions spontaneously aggregated into the ion pairs and quadrupoles shown in Fig. 2(b). This is an expected consequence of the ionophobic environment in C16O1and in accord with very low conductivities in C16O1:Li salt mixtures—too low to be measured using impedance spectroscopy [9]. Nonetheless, striking textures of liquid crystalline forms of Li salt 'complexes' of both C16O1 and a polyether–ester form, C16O1X (synthesised by dehydration of the diol analogous to i [9]) are observed at 50 °C, which is above the temperature (42 °C) at which both the pure polymers become isotropic. These liquid crystal forms demonstrate that the salts exert weak stabilising interactions on the polymers.

3.3. Conductivities

Figs. 3(a) and 4(a) show $\log \sigma$ versus $1/T$ plots for the four-component systems based upon C12C18O5X(18%) and C12C18O5Y(13%), respectively.. The data for each system are very similar. After the initial heating of the blended components to 110 °C the conductivities remain close to 10^{-3} S cm^{-1} during the first cooling down to ambient temperature. For the C12C18O5X(18%) system the deblended material is seen to be stable and precisely reproducible on the second thermal cycle. In the C12C18O5Y(13%) system the highest conductivities are achieved after two thermal cycles suggesting that the transformation or 'conversion' of the material that takes place at 110 °C is incomplete after the first heating, a phenomenon observed in other systems prepared by method Y. The result at 20 °C also falls slightly below the trend at higher temperatures. In the impedance data shown in Figs. 3(b) and 4(b) the sharp 'ticks' are indicative of 'liquid-like mobility' of ions but at 20 °C a change is apparent in both systems. The steeper slope in $\log \sigma$ versus $1/T$ below 20 °C is marked by the appearance of new arcs in the impedance plots. DSC shows an endotherm only at 26 °C with a shoulder at 16–18 °C. Thus, the steepening conductivity plot below 20 °C is tentatively attributable to crystallisation of polymer II although this is not certain at present. However, conductivities in the range 10^{-5} to 4×10^{-5} S cm^{-1} at −10 °C improve significantly on conventional amorphous systems for which such conductivities are generally observed at ca. 25 °C.

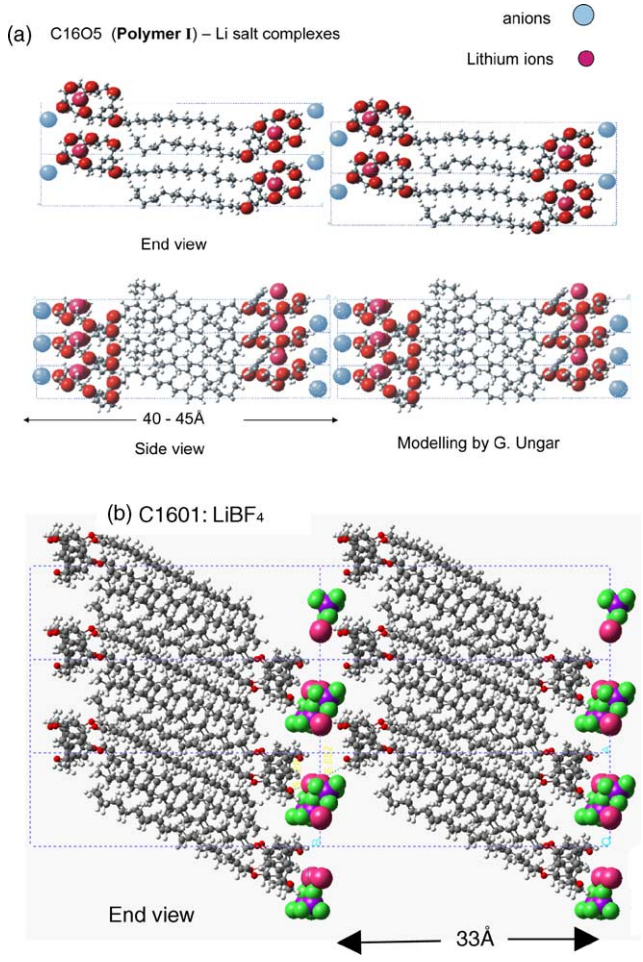

Fig. 2. Molecular dynamics models of low-dimensional polymer–Li salt complexes. (a) C16O5:Li salt (iodide) complex; (b) C16O1:$LiBF_4$ complex. Dark grey, carbon; light grey, hydrogen; red, oxygen; pink, Li^+; blue, anion (iodide); purple, boron; green, fluorine. Atoms not to scale.

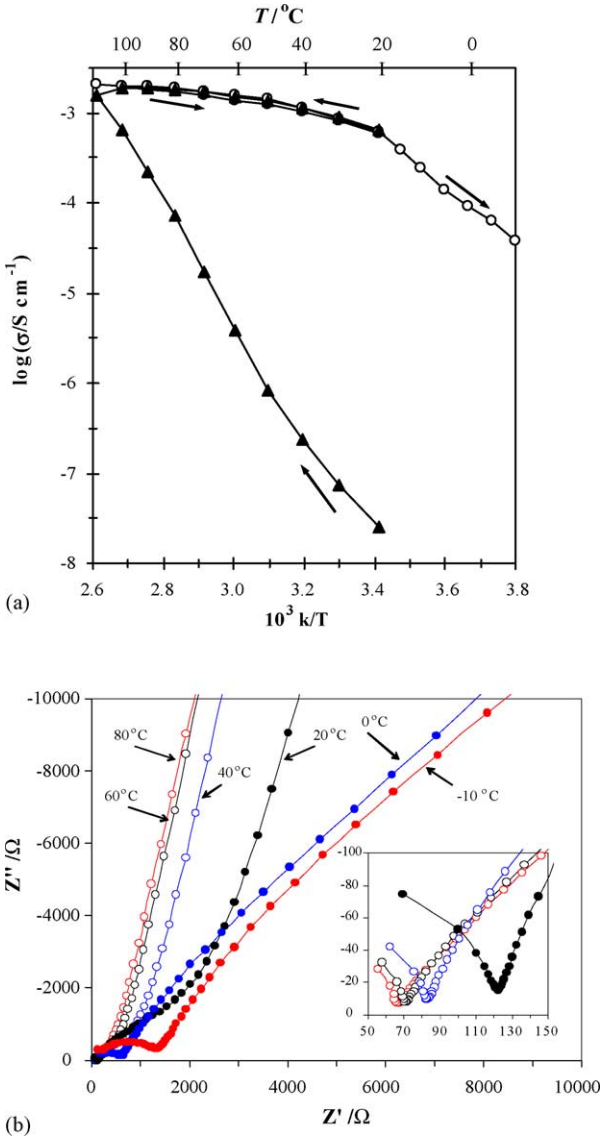

Fig. 3. Conductivity data for C12C18O5X(18%):II:III:$LiBF_4$ (1:0.8:0.2:1.2) (a) $\log\sigma$ vs. $1/T$; (▲) first thermal cycle; (◯) second cycle. (b) Impedance plots for second cycle. (Reproduced by permission of the Royal Society of Chemistry.)

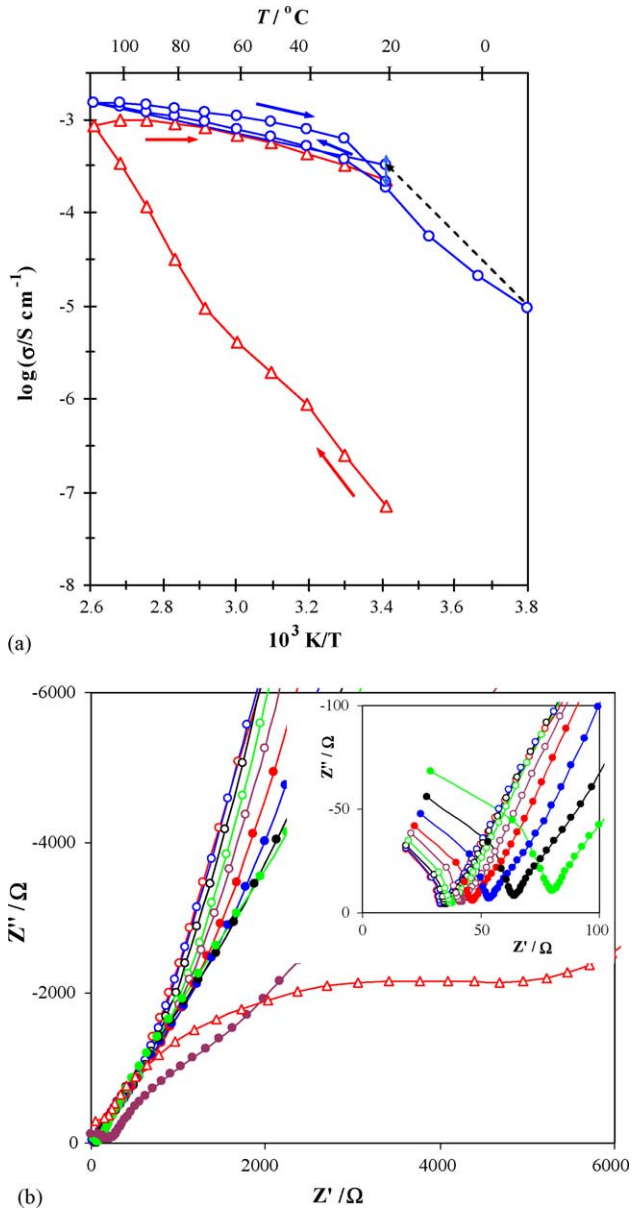

Fig. 4. (a) Conductivity data for C18C12O5Y(13%):II:III:$LiBF_4$ (1:0.8:0.2:1.2): arrows indicate direction of first (red) and second (blue) thermal cycles. (b) Impedance planes for second cooling and reheat to 20 °C: (○) 110 °C, (○) 100 °C, (○) 90 °C, (○) 80 °C, (○) 70 °C, (●) 60 °C, (●) 50 °C, (●) 40 °C, (●) 30 °C, (●) 20 °C and (△) −10 °C.

Furthermore, the close agreement at ambient temperatures between the ac impedance data and extended (48 h) dc polarisations [8] strongly suggest a predominance of Li^+ transport in the high conductivity low activation energy regime. Furthermore, preliminary ^{7}Li NMR studies by Apperley at the EPSRC facility, University of Durham, UK (to be published) also indicate significant Li mobility down to −20 °C in the C12C18O5Y(13%) system.

3.4. Mechanism of conduction

Prompted by the molecular modelling, we propose that the conduction process in the low temperature-dependent regime involves Li^+ hopping between decoupled neutral aggregates, e.g.,

$$\ldots Li_2A_2\ \ Li_3A_2{}^+\ Li_2A_2 \rightarrow Li_2A_2\ \ Li_2A_2\ \ Li_3A_2{}^+ \ldots$$

such as ion pairs or ‘quadrupoles’ (double ion pairs) as depicted in Fig. 5. Larger aggregates may be inhibited by the space available within the channels. SAXS data [9] in conjunction with molecular modelling indicates that the width of the channels may amount to approximately 10 Å being the separation imposed by a cation-filled loop of a tetraethoxy segment and its attendant anion. A quadrupole approximates to such a dimension and a larger aggregate may well be unstable.

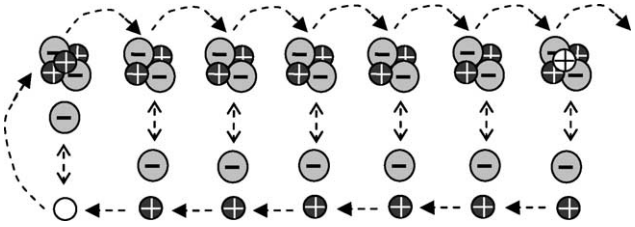

Fig. 5. A plausible mechanism for extended Li^+ transport along rows of decoupled neutral aggregates in a 'blocky' CmO1–CmO5 copolymer electrolyte. The parallel row of separated ions provides 'charge balancing' by local reorganisation.

However, 'cation-hopping' requires the mobile positive centre to be balanced by an anionic species. Cation mobility might be seriously impaired if the migrating cation were required to 'carry' an anion with it. C12C18O5Y(13%) was synthesised from pre-polymerised C12C18O5Y(82%) and C12C18O5Y(6%) so that the C12C18O5 and C12C18O1 units must be essentially sequenced in blocks allowing the possibility of parallel rows of aggregates and ion-separated pairs as shown in Fig. 5. Charge-balancing for left-to-right cation motion is achieved at all sites along the sequence of aggregates whilst in the ion-separated row the cations move only a single site right-to-left. 'Dis-proportionation' by disintegration of aggregates may also play a role. However, both syntheses X and Y may tend to engender 'block' sequencing both from the greater reactivity of the benzylic hydroxyls and from the heterogeneous nature of the reactions, from which less-soluble CmO1 sequences precipitate first and inhibit the access of tetraethylene glycol or its dibromide from immediate reaction.

Acknowledgements

We are grateful to the EPSRC and to the European Space Agency for support in this work.

References

[1] J.-M. Tarascon, M. Armand, Nature 414 (2001) 359–367.
[2] F.M. Gray, Polymer Electrolytes, Royal Society of Chemistry, Cambridge, UK, 1997, Chapters 5 and 6.
[3] P.E. Stallworth, J.J. Fontanella, M.C. Wintersgill, C.D. Scheidler, J.J. Immel, S.G. Greenbaum, A.S. Gozdz, J. Power Sources 81/82 (1999) 739–747.
[4] Y. Zheng, F. Chia, G. Ungar, P.V. Wright, Chem. Commun. (2000) 1459–1460.
[5] Y. Zheng, F. Chia, G. Ungar, P.V. Wright, J. Power Sources 97/98 (2001) 641–643.
[6] Y. Zheng, F. Chia, G. Ungar, P.V. Wright, Electrochim. Acta 46 (2001) 1397–1405.
[7] F. Chia, Y. Zheng, J. Liu, G. Ungar, P.V. Wright, Solid State Ionics 147 (2002) 275–280.
[8] F. Chia, Y. Zheng, J. Liu, N. Reeves, G. Ungar, P.V. Wright, Electrochim. Acta 48 (2003) 1939–1951.
[9] J. Liu, Y. Zheng, Y.-P. Liao, X. Zeng, G. Ungar, P.V. Wright, J. Chem. Soc. Faraday Transact. 128 (2005) 363–378.
[10] Y. Zheng, J. Liu, Y-P. Liao, X. Zeng, G. Ungar, P.V. Wright, J. Chem. Soc. Dalton Transact. (2004) 3053–3060.
[11] F.B. Dias, S.V. Batty, G. Ungar, J.P. Voss, P.V. Wright, J. Chem. Soc. Faraday Transact. 92 (1996) 2599–2606.